JOURNAL OF COMPUTATIONAL PHYSICS 40, 411–429 (1981)

An Asymptotic Outer Solution Applied to the Keller Box Method

EVERETT JONES

Department of Aerospace Engineering, University of Maryland, College Park, Maryland 20742

Received June 27, 1978; revised November 9, 1979

The Keller box method ("Numerical Solutions of Partial Differential Equations, Vol. 2" (B. Hubbard, Ed.), pp. 327–350, Academic Press, New York, 1970) was applied to incompressible flow past a flat plate to demonstrate that the basic computation region must extend outward from the wall until the outer boundary conditions are effectively obtained. The Keller box method was modified to include an asymptotic outer solution for the case of the self-similar solution for compressible flow in a boundary layer. Initial application of the basic and modified Keller box methods to incompressible flow past a flat plate showed similar rates of convergence but smaller RMS error for the same basic range of the independent variable when the asymptotic outer solution is applied. Furthermore, extension of the solution beyond the range of the independent variable for the numerical solution using the resulting asymptotic solution produced RMS error at least as small as the RMS error on the range of the numerical solution. Also, when the asymptotic solution was applied, a smaller range of independent variables could be used in the numerical solution to obtain the same RMS error. Numerical results for compressible flow were qualitatively the same as for the case with the incompressible velocity profile except the rate of iterative convergence was slightly slower. Application of asymptotic outer solution for incompressible flow at a two dimensional stagnation point produced similar results with smaller relative improvements. For compressible flow with smaller favorable pressure gradients than the stagnation point and with adverse pressure gradients, significant improvements were again obtained. Examination of the errors associated with the asymptotic solution reveals that greatest success is obtained for flows with thicker boundary layers and shows that the boundary layer at a two dimensional stagnation point is too thin for small error in the asymptotic solution. Despite relatively large errors in the asymptotic solutions for boundary layer in strong favorable pressure gradients where the boundary layer is thin, the boundary layer solutions generally showed improvement in error and reduction in computation times.

INTRODUCTION

The Keller box method [1] has become a popular method for obtaining non-similar solutions for boundary layer problems. The method has been extended [2] and compared with other techniques by Blottner [3, 4]. In this method, the system of partial differential equations for the viscous boundary layer are approximated on a rectangular net in physical or transformed coordinates. These approximate equations

0021-9991/81/040411-19$02.00/0

are linearized with all terms evaluated using values of the flow variables at the corners of each "box" in the rectangular net. As a result, the conservation equations for the boundary layer are reduced to a system of algebraic equations with the boundary conditions included. In the solution procedure, the solution must be known on an upstream cross section of the boundary layer and requires the solution of a system of algebraic equations, which is implicit with respect to variations normal to the boundary layer, at successive streamwise locations in the rectangular mesh.

The outer boundary conditions on the boundary layer are actually approached asymptotically and are only attained at large distances from the inner boundary. Therefore, the usual application of the outer boundary conditions at finite values of the normal coordinate as in Refs. [1–4] could produce significant error.

The asymptotic behavior of the boundary layer solution for large distances from the inner boundary is often of interest (as in the method of matched asymptotic expansions [5]) and will certainly be in error if the outer boundary conditions for a numerical solution are applied "too close" to the inner boundary. Consequently, inclusion of the asymptotic behavior in the Keller box method should give the resulting solution greater utility.

The purpose of the present investigation was twofold. First, the effect of applying the asymptotic outer boundary condition at finite distances from the surface was explored. Second, an outer asymptotic solution was incorporated into a numerical solution and its applicability was studied. For the preliminary analysis with asymptotic solution, the special case of a self-similar solution was treated as in [3, 4] in order to reduce computation times. Results for the basic Keller box method were sought in order to present rational comparisons.

The Basic Keller Box Method

The analytical development of the basic Keller box method is reviewed first since the exact method used to evaluate the sensitivity of calculations to the location of the outer boundary should be recorded. Furthermore, the modifications to the basic method due to the inclusion of the asymptotic solution were minor and only one complete presentation is necessary.

If temperature, $T(x, y)$, is non-dimensionalized with the edge temperature, $T_e(x)$, and the stream function, ψ, is introduced to satisfy conservation of mass identically, the velocity components, $u(x, y)$ and $v(x, y)$, and non-dimensionalized temperature, Θ, are given by

$$\rho u = \frac{\partial \psi}{\partial y}, \qquad \rho v = -\frac{\partial \psi}{\partial x}, \qquad \Theta(x, y) = T/T_e(x). \tag{1}$$

Then, the parallel and normal coordinates, x and y, and the stream function can be transformed with

$$\xi = \kappa \int_0^x (\rho\mu)_R \, u_e \, dx, \qquad \eta = \frac{u_e}{g(\xi)} \int_0^y \rho \, dy, \tag{2}$$

$$\psi(x, y) = g(\xi) \, f(\xi, \eta), \qquad g(\xi) = \sqrt{2\xi C_\eta / \kappa}, \tag{3}$$

which reduces the equations for conservation of momentum and energy with a calorically perfect gas to

$$\frac{\partial}{\partial \eta}\left(\frac{F}{C_\eta}\frac{\partial^2 f}{\partial \eta^2}\right) + f\frac{\partial^2 f}{\partial \eta^2} + \beta\left[\Theta - \left(\frac{\partial f}{\partial \eta}\right)^2\right] = 2\xi\left(\frac{\partial f}{\partial \eta}\frac{\partial^2 f}{\partial \xi \, \partial \eta} - \frac{\partial f}{\partial \xi}\frac{\partial^2 f}{\partial \eta^2}\right), \tag{4}$$

$$\frac{\partial}{\partial \eta}\left(\frac{F}{P_R C_\eta}\frac{\partial \Theta}{\partial \eta}\right) + f\frac{\partial \Theta}{\partial \eta} + \frac{F\alpha}{C_\eta}\left(\frac{\partial^2 f}{\partial \eta^2}\right)^2 = 2\xi\left(\frac{\partial f}{\partial \eta}\frac{\partial \Theta}{\partial \xi} - \frac{\partial f}{\partial \xi}\frac{\partial \Theta}{\partial \eta}\right), \tag{5}$$

where

$$F = (\rho\mu)/(\rho\mu)_R, \qquad \alpha = \frac{u_e^2}{C_p T_e} = (\gamma - 1) M^2, \tag{6}$$

$$\beta = \frac{2\xi}{u_e}\frac{du_e}{d\xi} = \text{pressure gradient parameter}, \qquad P_R = \frac{\mu C_p}{k}. \tag{7}$$

κ is the usual constant in the boundary layer transformation but C_η is a new constant introduced in order to make the coefficients of the incompressible form of (4) and (5) consistent with the differential equations for known exact solutions. $(\rho\mu)_R$ denotes a reference density–viscosity product which is normally the wall or edge value. The appropriate boundary conditions are

$$0 = f(\xi, 0) = \frac{\partial f}{\partial \eta}(\xi, 0), \qquad \Theta(\xi, 0) = \Theta_w \qquad \text{or} \qquad \frac{\partial \Theta}{\partial \eta}(\xi, 0) = \Theta'_w, \tag{8}$$

$$\frac{\partial f}{\partial \eta}(\xi, \eta) = f'_\infty, \qquad \Theta(\xi, \eta) = \Theta_\infty \text{ as } \eta \text{ becomes infinite.} \tag{9}$$

For this exploratory analysis, the self-similar solution (f and Θ as functions of η only) was sought such that the right sides of (4) and (5) are zero and these equations become ordinary differential equations. The first step of the box method applied to this problem is to create a system of first order equations by introducing the new variables, U, V and W, defined as follows:

$$f' = U, \qquad f'' = U' = V, \qquad \Theta' = W. \tag{10}$$

An iteration procedure is used to solve the system of equations. The superscript i indicates the quantity for the ith iteration with

$$\begin{aligned} f^i &= f^{i-1} + \delta_f^i, \qquad U^i = U^{i-1} + \delta_U^i, \qquad V^i = V^{i-1} + \delta_V^i, \\ \Theta^i &= \Theta^{i-1} + \delta_\Theta^i, \qquad W^i = W^{i-1} + \delta_W^i, \end{aligned} \tag{11}$$

where δ_f^i, δ_U^i, δ_V^i, δ_Θ^i and δ_W^i are the ith iterates for f, U, V, Θ, and W and will produce "small" changes if the procedure converges. For the present compressible case, the function $F(\Theta)$ was expanded in a Taylor's series such that

$$F^i \equiv F(\Theta^i) = F(\Theta^{i-1}) + F'(\Theta^{i-1})\,\delta_\Theta^i = F^{i-1} + (F')^{i-1}\,\delta_\Theta^i. \tag{12}$$

The computational mesh was defined by

$$\eta_j = \eta_{j-1} + (\Delta\eta)_j \qquad \text{for} \quad j = 2, 3, \ldots, J, \tag{13}$$

where $\eta_1 = 0$ and $\eta_J = \eta_{\max}$. The Prandtl number was assumed to be constant and central differences are introduced at the midpoints of the mesh, $\eta_{j-1/2} = \frac{1}{2}(\eta_j + \eta_{j-1})$ such that (4), (5) and (10) become

$$-\delta_{f_{j-1}}^i + \delta_{f_j}^i - \frac{(\Delta\eta)_j}{2}\,\delta_{U_{j-1}}^i - \frac{(\Delta\eta)_j}{2}\,\delta_{U_j}^i = \frac{(\Delta\eta)_j}{2}\,(U_j^{i-1} + U_{j-1}^{i-1}) - (f_j^{i-1} - f_{j-1}^{i-1}), \tag{14}$$

$$-\delta_{U_{j-1}}^i + \delta_{U_j}^i - \frac{(\Delta\eta)_j}{2}\,\delta_{V_{j-1}}^i - \frac{(\Delta\eta)_j}{2}\,\delta_{V_j}^i = \frac{(\Delta\eta)_j}{2}\,(V_j^{i-1} + V_{j-1}^{i-1}) - (U_j^{i-1} - U_{j-1}^{i-1}), \tag{15}$$

$$\tilde{a}_j\delta_{f_{j-1}}^i + a_j\delta_{f_j}^i + \tilde{b}_j\delta_{U_{j-1}}^i + b_j\delta_{U_j}^i + \tilde{c}_j\delta_{V_{j-1}}^i + c_j\delta_{V_j}^i + \tilde{d}_j\delta_{\Theta_{j-1}}^i + d_j\delta_{\Theta_j}^i = s_j, \tag{16}$$

$$-\delta_{\Theta_{j-1}}^i + \delta_{\Theta_j}^i - \frac{(\Delta\eta)_j}{2}\,\delta_{W_{j-1}}^i - \frac{(\Delta\eta)_j}{2}\,\delta_{W_j}^i = \frac{(\Delta\eta)_j}{2}\,(W_j^{i-1} + W_{j-1}^{i-1}) - (\Theta_j^{i-1} - \Theta_{j-1}^{i-1}), \tag{17}$$

$$\tilde{\alpha}_j\delta_{f_{j-1}}^i + \alpha_j\delta_{f_j}^i + \tilde{\beta}_j\delta_{V_{j-1}}^i + \beta_j\delta_{V_j}^i + \tilde{\gamma}_j\delta_{\Theta_{j-1}}^i + \gamma_j\delta_{\Theta_j}^i + \tilde{\zeta}_j\delta_{W_{j-1}}^i + \zeta_j\delta_{W_j}^i = t_j, \tag{18}$$

where the undefined coefficients depend upon the method used to evaluate the product terms.

As in [4], one technique for calculating the product terms, which will be designated by $l = 0$, is

$$(fV)_{j-1/2} = \tfrac{1}{2}[(fV)_j + (fV)_{j-1}] = \tfrac{1}{2}[f_jV_j + f_{j-1}V_{j-1}] \tag{19}$$

such that a product at the midpoint is evaluated as the average of the products at the neighboring mesh points. An alternative technique for calculating the product terms will be designated by $l = 1$ and applies

$$(fV)_{j-1/2} = f_{j-1/2}V_{j-1/2} = \tfrac{1}{4}(f_j + f_{j-1})(V_j + V_{j-1}). \tag{20}$$

Here the product at the midpoint is evaluated as the product of the midpoint values. The form of (19) and (20) was extended to all product terms.

The boundary conditions from (8) become

$$\delta_{f_1}^i = 0 = \delta_{U_1}^i, \qquad f_1^0 = 0 = U_1^0, \tag{21}$$

$$(1-m)\,\delta_{\Theta_1}^i + m\delta_{W_1}^i = 0, \qquad (1-m)(\Theta_1^0 - \Theta_w) + m(W_1^0 - \Theta_w') = 0, \tag{22}$$

where $m = 0$ reduces (22) to the wall temperature condition and $m = 1$ yields the wall flux condition. For the basic Keller box method, the outer boundary conditions are applied at the outermost mesh point, $\eta = \eta_{\max}$ or $j = J$, with

$$\delta^i_{U_J} = 0 = \delta^i_{\Theta_J}, \qquad U^0_J = f'_\infty, \qquad \Theta^0_J = \Theta_\infty. \tag{23}$$

This system of equations has five equations for each j and forms a linear, block tridiagonal matrix which can be solved efficiently [2].

The outer boundary conditions in (9) are only approached asymptotically for very large η. However, calculations will be more economical if $\eta_{\max}$ is reduced. As will be shown later, considerable error can result if $\eta_{\max}$ is reduced "too much" for the basic box method. Therefore, incorporation of an asymptotic behavior can be advantageous.

The Keller Box Method with Asymptotic Outer Solution

Since the boundary conditions in (9) are approached asymptotically, $F(\Theta)$ approaches $F_\infty = F(\Theta_\infty)$ asymptotically. In a manner similar to the original Blasius solution for a flat plate [6] the form chosen for an asymptotic solution is

$$f(\eta) = (f'_\infty \eta + A) + f_1(\eta), \qquad A = \text{a constant}, \tag{24}$$

$$\Theta(\eta) = \Theta_\infty + \Theta_1(\eta), \qquad F(\Theta) = F_\infty + F'(\Theta_\infty)\,\Theta_1(\eta), \tag{25}$$

where the leading terms are assumed to be much larger than the next terms in each equation. Substitution of (24) and (25) into (4) and (5) and neglect of the nonlinear terms yields

$$0 = \frac{1}{C_\eta} F_\infty f'''_1 + (f'_\infty \eta + A) f''_1 + \beta[\Theta_1 - 2f'_\infty f'_1], \tag{26}$$

$$0 = \frac{1}{C_\eta} \frac{F_\infty}{P_{R_\infty}} \Theta''_1 + (f'_\infty \eta + A)\,\Theta'_1. \tag{27}$$

As η becomes infinite, asymptotic approach to the boundary conditions in (9) requires that f_1 and Θ_1 and their derivatives become zero.

Equation (27) is a linear equation for Θ'_1. Its solution subject to the outer boundary conditions produces

$$\Theta(\eta) = \Theta_\infty + B \operatorname{erfc} \xi,$$
$$\xi \equiv \alpha_\xi (f'_\infty \eta + A), \qquad \alpha^2_\xi = (C_\eta P_{R_\infty})/(2F_\infty f'_\infty), \tag{28}$$

where

$$\operatorname{erfc} \xi = \text{the complementary error function} = (2/\sqrt{\pi}) \int_\xi^\infty e^{-t^2}\, dt.$$

The inhomogeneous term in (26) is a function of ξ and will be proportional to B. Furthermore, the asymptotic outer boundary conditions require that the complementary solution will have only one arbitrary constant. Therefore, the solution for $f_1(\eta)$ will have the form

$$f_1(\eta) = G(\xi) = BG_p(\xi) + CG_c(\xi), \tag{29}$$

which reduces (26) to

$$L(G) \equiv G''' + \frac{2}{P_{R_\infty}} \xi G'' - \frac{4\beta}{P_{R_\infty}} G' = \frac{-2\beta B}{\alpha_\xi P_{R_\infty} (f'_\infty)^2} \operatorname{erfc} \xi. \tag{30}$$

The solution of (30) has two special cases. When the pressure gradient is zero ($\beta = 0$), (30) is homogeneous and has an exact solution with

$$G_c(\xi) = (2\pi^{1/2}/P_{R_\infty})\, i^1 \operatorname{erfc}(\xi/P_{R_\infty}^{1/2}), \qquad G_p(\xi) = 0, \tag{31}$$

where

$$i^1 \operatorname{erfc} \xi \equiv \int_\xi^\infty \operatorname{erfc} \xi \, d\xi.$$

When the pressure gradient is nonzero, a series solution for $G_c(\xi)$ and its derivatives is given by

$$\begin{aligned} G_c(\xi) &= e^{-\xi^2/P_{R_\infty}} \sum_{i=0}^{\infty} A_i \xi^{-2(i+1+\beta)}, \\ G'_c(\xi) &= \frac{-2}{P_{R_\infty}} e^{-\xi^2/P_{R_\infty}} \sum_{i=0}^{\infty} B_i \xi^{-(1+2\beta+2i)}, \end{aligned} \tag{32}$$

$$\begin{aligned} G''_c(\xi) &= \left(\frac{2}{P_{R_\infty}}\right)^2 e^{-\xi^2/P_{R_\infty}} \sum_{i=0}^{\infty} C_i \xi^{-2(1+\beta)}, \\ G'''_c(\xi) &= -\left(\frac{2}{P_{R_\infty}}\right)^3 e^{-\xi^2/P_{R_\infty}} \sum_{i=1}^{\infty} D_i \xi^{(1-2\beta-2i)}, \end{aligned} \tag{33}$$

where

$$A_0 = B_0 = 1 = C_0 = D_0, \tag{34}$$

$$B_i = \left\{(i+\beta)[1-2(i+\beta)] \frac{P_{R_\infty}}{2i}\right\} B_{i-1}, \qquad A_i = B_i - P_{R_\infty}(i+\beta) A_{i-1}, \tag{35}$$

$$C_i = \frac{P_{R_\infty}}{2i} [1-2(i+\beta)] B_{i-1}, \qquad D_i = C_i - P_{R_\infty}[1-(1+\beta)] C_{i-1}. \tag{36}$$

For the special case of unit Prandtl number,

$$G_p(\xi) = -(\operatorname{erfc}\xi)/[2\alpha_\xi (f'_\infty)^2]. \tag{37}$$

When P_{R_∞} is not unity, it is convenient to introduce

$$G_p(\xi) = \beta F_p(\xi)/[4\pi^{1/2}\alpha_\xi (f'_\infty)^2 (P_R - 1)] \tag{38}$$

and the asymptotic solution for erfc ξ such that the series solution for $F_p(\xi)$ is

$$F_p(\xi) = e^{-\xi^2} \sum_{i=0}^{\infty} A_i \xi^{-2(2+i)}, \qquad F'_p(\xi) = -2e^{-\xi^2} \sum_{i=0}^{\infty} B_i \xi^{-(3+2i)}, \tag{39}$$

$$F''_p(\xi) = e^{-\xi^2} \sum_{i=0}^{\infty} C_i \xi^{-2(1+i)}, \qquad F'''_p(\xi) = -8e^{-\xi^2} \sum_{i=0}^{\infty} D_i \xi^{-(1+2i)}, \tag{40}$$

$$A_0 = B_0 = 1 = C_0 = D_0,$$

$$E_0 = 1, \qquad E_m = (-1)^m \frac{1 \cdot 3 \cdot 5 \cdots (2m-1)}{2^m} \qquad \text{for} \quad m > 0, \tag{41}$$

$$C_i = E_i + \frac{P_{R_\infty}}{1 - P_{R_\infty}} \left[iC_{i-1} - \frac{\beta}{P_{R_\infty}} B_{i-1} \right], \quad B_i = C_i - \frac{(2i+1)}{2} B_{i-1}, \tag{42}$$

$$A_i = B_i - (1+i) A_{i-1}, \quad D_i = C_i + iC_{i-1}. \tag{43}$$

Equations (24), (28) and (29) with (31) to (43) give the asymptotic solution for f, $U = f'$, $V = f''$, Θ, $W = \Theta'$ with three arbitrary coefficients (A, B and C). Specification of the coefficients completes the asymptotic solution and these coefficients must be determined as part of the iterative solution. Assuming that the coefficients also change little between iterations, this asymptotic solution can be employed to find the ith iterates of the basic Keller box method at the outermost η as follows:

$$\begin{aligned}
\delta^i_{f_J} &= \left(\frac{\partial f}{\partial A}\right)^{i-1}_J \delta^i_A + \left(\frac{\partial f}{\partial B}\right)^{i-1}_J \delta^i_B + \left(\frac{\partial f}{\partial C}\right)^{i-1}_J \delta^i_C, \\
\delta^i_{U_J} &= \left(\frac{\partial U}{\partial A}\right)^{i-1}_J \delta^i_A + \left(\frac{\partial U}{\partial B}\right)^{i-1}_J \delta^i_B + \left(\frac{\partial U}{\partial C}\right)^{i-1}_J \delta^i_C, \\
\delta^i_{V_J} &= \left(\frac{\partial V}{\partial A}\right)^{i-1}_J \delta^i_A + \left(\frac{\partial V}{\partial B}\right)^{i-1}_J \delta^i_B + \left(\frac{\partial V}{\partial C}\right)^{i-1}_J \delta^i_C,
\end{aligned} \tag{44}$$

$$\delta^i_{\Theta J} = \left(\frac{\partial \Theta}{\partial A}\right)^{i-1}_J \delta^i_A + \left(\frac{\partial \Theta}{\partial \beta}\right)^{i-1}_J \delta^i_B, \tag{45}$$

$$\delta^i_{W_J} = \left(\frac{\partial W}{\partial A}\right)^{i-1}_J \delta^i_A + \left(\frac{\partial W}{\partial B}\right)^{i-1}_J \delta^i_B, \tag{46}$$

where

$$\delta_A^i = A^i - A^{i-1}, \qquad \delta_B^i = B^i - B^{i-1}, \qquad \delta_C^i = C^i - C^{i-1}. \tag{47}$$

Equations (44) to (47) were used to replace the five ith iterates (δ_f^i, δ_U^i, δ_V^i, δ_Θ^i, and δ_w^i) by the three iterates (δ_A^i, δ_B^i, and δ_C^i) as unknowns at the outermost η (i.e., $j = J$) in the block matrix for the basic box method. As a result, a new block tridiagonal matrix is obtained for the $\delta_{f_j}^i$, $\delta_{U_j}^i$, $\delta_{V_j}^i$, $\delta_{\Theta_j}^i$, and $\delta_{w_j}^i$ for all $j < J$ and also for the δ_A^i, δ_B^i, and δ_C^i.

Numerical Results and Discussion

One factor of interest is the rate of convergence of the modified box method and the basic Keller box method. The variation of wall stress from one iteration to the next iteration is the convergence test used by many investigators. However, the entire profile, particularly the profile at large η, is of interest here and the parameter used was

$$(\text{RMS Deviation})^i = \left\{ \frac{1}{J} \sum_{j=1}^{J} \left[(\delta_{f_j}^i)^2 + (\delta_{U_j}^i)^2 + (\delta_{V_j}^i)^2 + (\delta_{\Theta_j}^i)^2 + (\delta_{W_j}^i)^2 \right] \right\}^{1/2}. \tag{48}$$

Additional parameters of interest for the incompressible flow cases where the exact solutions exist are

$$(\text{RMS Error in } f, f' \text{ and } f'')^i = \left\{ \frac{1}{N} \sum_{j=1}^{N} \left[(f^i - f_{\text{EXACT}})_j^2 + (U^i - f'_{\text{EXACT}})_j^2 + (V^i - f''_{\text{EXACT}})_j^2 \right] \right\}^{1/2}, \tag{49}$$

$$(\text{RMS Error in } \Theta \text{ and } \Theta')^i = \left\{ \frac{1}{N} \sum_{j=1}^{N} \left[(\Theta^i - \Theta_{\text{EXACT}})_j^2 + (W - \Theta'_{\text{EXACT}})_j^2 \right] \right\}^{1/2}, \tag{50}$$

where N is the number of η values in the table for the exact solution. Also

$$(\text{RMS Error in } f, f', f'', \Theta \text{ and } \Theta')^i = \{ [\text{RMS Error in } f, f' \text{ and } f'')^i]^2 + [(\text{RMS Error in } \Theta \text{ and } \Theta')^i]^2 \}^{1/2}. \tag{51}$$

The solution for incompressible flow past a flat plae is well known [7] and was used as a basic test of the solution procedures. The flat plate solution for f is readily obtained from the present procedure with $\beta = 0$ and $F(\Theta) = 1$. Then (4) becomes decoupled from (5) and with $C_\eta = \frac{1}{2}$ the usual boundary value problem for f with incompressible flow is obtained.

In these exploratory calculations, a constant mesh size, $(\Delta\eta)_j = 0.2$, was chosen to allow direct comparison with the tabulation of the exact solution for an incompressible flat plate [7]. Furthermore, the condition $P_R = 1$ was imposed so the exact (Crocco) solution for temperature could be extracted directly from the exact velocity solution with

$$(\Theta) = \Theta_\infty + (f'_\infty - f')[(\alpha/2) f'_\infty (f'_\infty + f') - C_w], \tag{52}$$

where

$$C_w = [(\Theta_\infty - \Theta_w + (\alpha/2) f']/f'_\infty \qquad \text{when} \quad m = 0$$
$$= \Theta'_w/f''(0) \qquad \text{when} \quad m = 1.$$

Initial profiles ($i = 0$) are necessary to start the iteration process. For the present calculation, a procedure very similar to that of Blasius [6] is followed. The asymptotic solutions of (24) and (28) to (43) were joined to polynomials for f and Θ at small η. By equating f, f' and Θ at a selected value of ξ, relations between the arbitrary coefficients of the inner and outer solutions were obtained. The outer

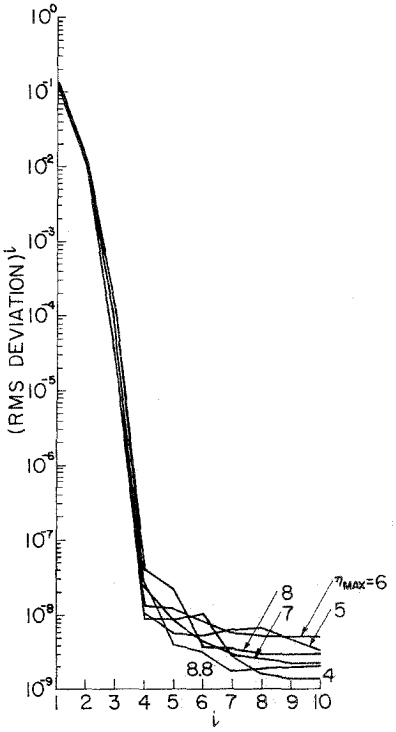

FIG. 1. The RMS deviation for the incompressible flat plate flow using the basic Keller box method with the infinity boundary conditions applied at η of η_{max} for a constant wall temperature of ($m = 0$), $l = 1$, $\gamma = 1.4$, $M = 4$, $F = 1 = P_R$ and $\beta = 0$.

boundary conditions are included in (28) and (29) and the wall boundary conditions were then applied to evaluate the coefficients of the polynomials. This matching process produces the coefficients of the polynomials and the initial values of the coefficients for the asymptotic solution (A^0, B^0 and C^0).

Figures 1 to 6 present results for $\gamma = 1.4$, $M = 4$, $F(\Theta) = l = 1 = P_R(\Theta)$, and $\beta = 0 = m$ (with $\Theta_w = 1$). This wall temperature condition was chosen since the resulting temperature profile will have a maximum which should provide a non-trivial test of the method. From Fig. 1, it is apparent that the rate of convergence of the basic Keller box method is virtually independent of $\eta_{\max}$. Since the tabulations for the exact solution [7] show that f and its derivatives vary quite rapidly in the region of $\eta = 4$ and $f' > 0.99$ only for $\eta > 4.9$, it was surprising that the method converges so rapidly for $\eta_{\max} = 4$. Note that the common definition of boundary layer thickness is the value of y where $f' = 0.99$.

The RMS error in f, f', f'', Θ and Θ' shown in Fig. 2 is greater than 50% for

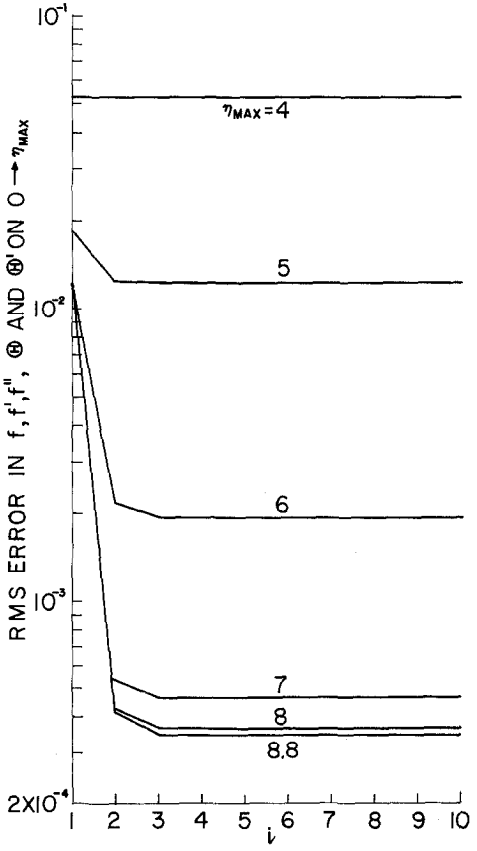

FIG. 2. The RMS error in the velocity and temperature profiles for the incompressible flat plate flow using the basic Keller box method with the infinity boundary conditions applied at η of $\eta_{\max}$ for a constant wall temperature ($m = 0$), $l = 1$, $\gamma = 1.4$, $M = 4$, $N = J$, $F = 1 = P_R$ and $\beta = 0$.

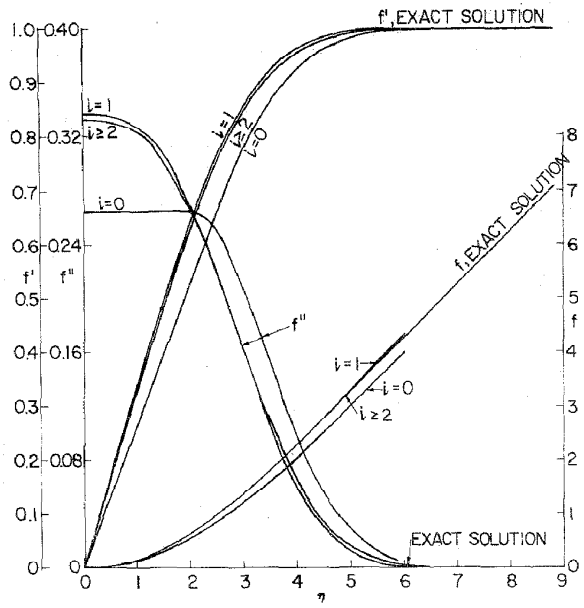

FIG. 3. The velocity profile for the incompressible flat plate flow using the basic Keller box method with the infinity boundary conditions applied at η_{max} of 6 for a constant wall temperature ($m = 0$), $l = 1$, $\gamma = 1.4$, $M = 4$ and $F = 1 = P_R$.

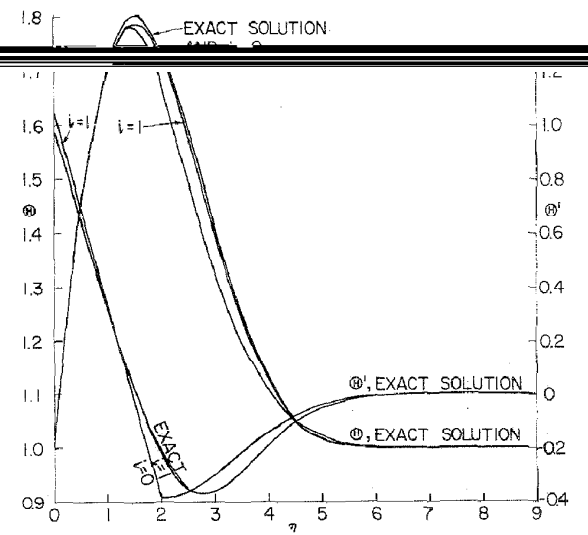

FIG. 4. The temperature profile for the incompressible flat plate flow using the basic Keller box method with infinity boundary conditions applied at η_{max} of 6 for constant wall temperature ($m = 0$), $l = 1$, $\gamma = 1.4$, $M = 4$, and $F = 1 = P_R$.

$\eta_{max} = 4$. With increasing η_{max}, the accuracy improves and for $\eta_{max} \geqslant 6$, the accuracy increased rapidly for increasing i with the best accuracy essentially attained by the third iteration. For $\eta_{max} = 6$, the velocity and temperature profiles shown in Figs. 3 and 4 effectively converge to the exact solution by the second iteration. It is apparent that reasonable accuracy is not obtained unless η_{max} is sufficiently large that the outer boundary condition is effectively attained even though iterative convergence may be obtained for much smaller η_{max}.

Figures 5 and 6 present comparable results for the modified Keller box method with asymptotic solution. From Fig. 5, it would appear that this method does not converge as rapidly, particularly for the cases with smaller η_{max}. Figure 6 presents the RMS error on the complete range of the tabulation ($0 \leqslant \eta \leqslant 8.8$). For $\eta_{max} < 8.8$, the computed values were extended using the asymptotic solutions. Comparisons of the RMS error in Figs. 2 and 6 shows that inclusion of the asymptotic solution will produce a solution which is as accurate as a solution from the original box method with significantly larger η_{max}. Also the asymptotic solution was successfully applied to extend he solution to the outer limit of the tabulated exact solution for the velocity profile [6]. The velocity and temperature profiles with asymptotic solution effectively

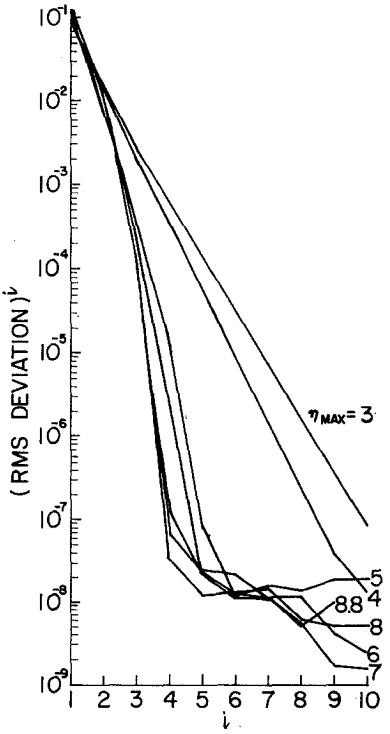

FIG. 5. The RMS deviation for the incompressible flat plate flow using the modified Keller box method with the asymptotic solution applied for $\eta \geqslant \eta_{max}$, constant wall temperature ($m = 0$), $\gamma = 1.4$, $M = 4$ and $F = 1 = P_R$.

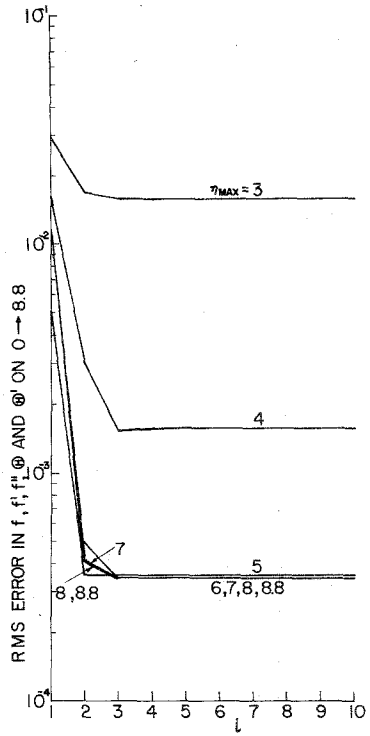

FIG. 6. The RMS error in the velocity and temperature profiles for the incompressible flat plate flow using the modified Keller box method with the asymptotic solution applied for $\eta \geqslant \eta_{max}$, constant wall temperature ($m = 0$), $l = 1$, $\gamma = 1.4$, $M = 4$, $N = J$ and $F = 1 = P_R$.

converge to the exact solution by the third iteration for a value of $\eta_{max} = 4$, where the basic Keller box method is not accurate.

Results were also obtained for the same flow ($\gamma = 1.4$, $M = 4$, $\beta = 0$, $F(\Theta) = 1 = P_R$, and $\Theta_w = 1$) with the alternate algorithm ($l = 0$). The rate of convergence for the basic and modified box methods were very close to the results shown in Figs. 1 and 5. Also, the RMS errors were qualitatively the same but the errors for the converged solutions were larger. The velocity and temperature profiles were in agreement with the profiles of the previous case ($l = 1$) except that the algorithm with $l = 0$ does not have as smooth an iterative convergence for the velocity profile since the deviations for the first iteration are larger.

The RMS error for the converged solutions with l of 0 and 1 are compared in Fig. 7. For the RMS error on the range of the exact solution (0 to 8.8), the solutions with the basic Keller box method are extended from η_{max} to 8.8 with the obvious choice

$$f'' = 0, \quad f' = 1, \quad f = f(\eta_{max}) + f'_\infty(\eta - \eta_{max}), \quad \Theta' = 0, \quad \Theta = \Theta_\infty. \tag{53}$$

It is apparent that the solution with outer asymptotic solution is better than the solution with the original box method for small η_{max}. The asymptotic solution significantly improves accuracy for η_{max} less than 6 when $l = 0$ and for η_{max} less than 7 when $l = 1$. However, the algorithm with $l = 0$ produces much larger error for both methods.

Next, the adiabatic wall boundary condition ($\Theta'_w = 0$ with $m = 1$) was applied to the same incompressible flow with $\beta = 0$, $\gamma = 1.4$, $M = 4$, and $F(\Theta) = 1 = P_R(\Theta)$ using the more accurate algorithm ($l = 1$). The RMS deviations and errors were qualitatively the same as the previous results for this algorithm. The velocity and temperature profiles also converged in virtually identical iterations. The RMS errors for the converged solutions in Fig. 8 are qualitatively the same as the previous results in Fig. 7 but the error at larger η_{max} is approximately a factor of 2 larger.

For a final test case with the flat plate the compressible flow of a perfect gas with $\gamma = 1.4$, constant coefficient of viscosity so $F(\Theta) = 1/\Theta$, $P_R = 1$, $M = 4$, constant wall temperature $\Theta_w = 1$, and $l = 0$ (the least accurate algorithm) was considered. Since a well documented solution was not available, the solution from the modified Keller box method for $\eta_{max} = 8.8$ was used as the "standard" of comparison replacing the exact solution to compute an RMS difference (instead of error) using (51). The major difference between these results and the previous results is that convergence is a little slower for larger η_{max}. The convergence of the velocity and temperature profiles showed larger difference between iterations but practical convergence which is essentially as rapid as that for the previous case.

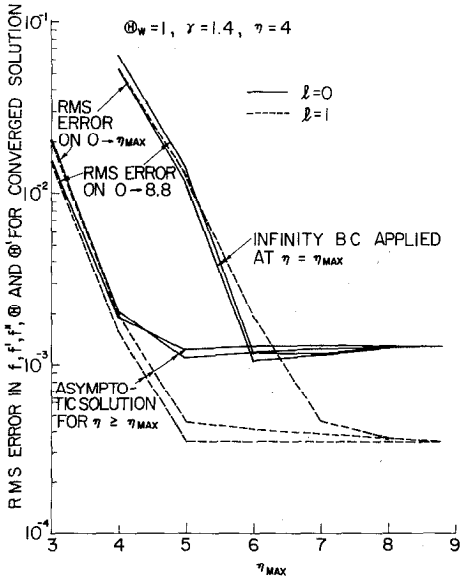

FIG. 7. Comparison of the RMS errors in the converged solution for the incompressible flat plate flow using the basic and modified box methods with constant wall temperature ($m = 0$), $\gamma = 1.4$, $M = 4$ and $F = 1 = P_R$ for $l = 0$ and 1 on the computation region (0 to η_{max}) and the extended region (0 to 8.8).

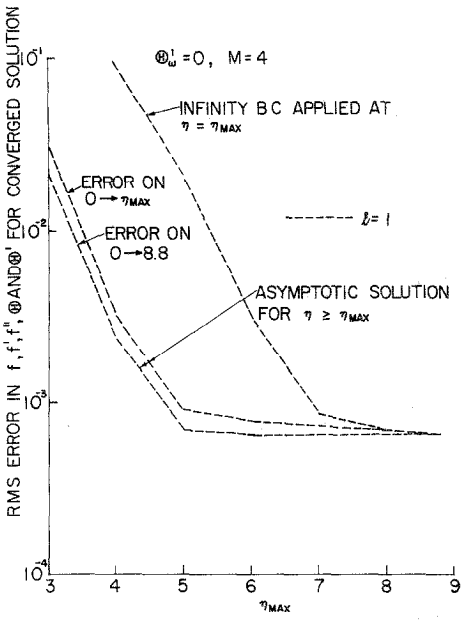

FIG. 8. Comparison of the errors in the converged solution for the incompressible flat plate using the basic and modified box methods with adiabatic wall ($m = 1$), $\gamma = 1.4$, $M = 4$ and $F = 1 = P_R$ for $l = 1$ on the computation region (0 to η_{max}) and the extended region (0 to 8.8).

The rate of convergence of the modified box method for this case is also somewhat slower than for previous cases. The velocity and temperature profiles with η_{max} of 4 converged in a manner very similar to that for the basic Keller box method with $\eta_{max} = 6$ except that a discontinuity in the profiles for f'' and θ' exists for the first iteration with the modified box method and that convergence is slightly faster.

The programs for the two algorithms compared here included several features considered important for the comparisons. Even though programming efficiency was not of prime importance, the programs had the same features and relative comparisons of computer times has significance. For the sample cases reported, inclusion of the asymptotic outer solution with η_{max} of 6 increased computer time by 6.7% for 10 iterations. However, reduction of the η_{max} with the asymptotic outer solution to 4 reduces computer time by 25.6% for 10 iterations with negligible sacrifice in accuracy or rate of convergence. As a result, a net savings in computer time was obtained.

Incompressible flow past a two dimensional stagnation point has a well-known exact, self-similar solution including the pressure gradient [7]. Equation (4) reduces to the ordinary differential equation for this problem with the following choice of parameters:

$$F = 1 = C_\eta = \beta \tag{54}$$

and

$$\Theta = 1.0. \tag{55}$$

The slight modification of the outer asymptotic solution

$$f = f'_\infty \left[\eta - \frac{1}{\sqrt{2}} + i^1 \operatorname{erfc} \eta\right]$$

for an initial profile. For this case, imposition of

$$P_R = 1, \qquad \alpha = 0, \tag{56}$$

and (54) reduces the energy equation to

$$\frac{d^2\Theta}{d\eta^2} + f\frac{d\Theta}{d\eta} = 0. \tag{57}$$

With $\Theta_w = \Theta_\infty$,

$$\Theta(\eta) = \Theta_w = \Theta_\infty = 1 \tag{58}$$

will be a reasonable initial profile and should be the exact solution.

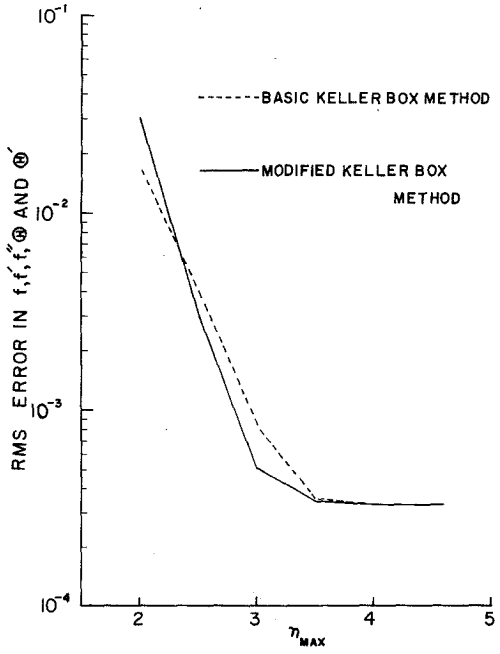

FIG. 9. The RMS errors in the converged velocity profile on the interval $0 \leqslant \eta \leqslant 4.6$ for incompressible flow at a two dimensional stagnation point with $\gamma = 1.4$, $M = 0$, $f'_\infty = 1 = P_R = \Theta_\infty = \Theta_w = \beta = l = C_n = F_\infty$.

Exercise of the modified programs to include the conditions in (54) to (56) produced the results shown in Fig. 9 for the RMS error in the velocity profile computed using (49). These computations used $\Delta\eta$ of 0.1 but were only compared to the exact solution at the tabulated values of η in [7], i.e., for $\Delta\eta$ of 0.1 for η up to 2.0 and $\Delta\eta$ of 0.2 from 2.0 to the maximum value of 4.6. For $\eta_{max} \geqslant 3.5$, there is negligible difference in the error of either method, and for $2.3 \leqslant \eta_{max} \leqslant 3.5$, the modified method is somewhat better. At smaller η_{max} the error for both methods is rapidly becoming too large. As expected (58) was essentially the exact solution since the maximum RMS difference of the computed solution and (58) for the η_{max} of Fig. 9 was zero for the basic Keller box method and 0.67×10^{-7} for the modified Keller box method.

The exact solution [6] has $f' > 0.99$ for $\eta > 2.3$. Hence the boundary layer thickness is the value of y obtained at this value of η. It is interesting to note that the RMS error of the computed solutions does not become independent of the η_{max} used until somewhat larger values are used.

Solutions were obtained for compressible flow with pressure gradients with $\beta = 0.5$ and -0.1. The RMS differences of the velocity and temperature profiles for these cases are shown on Fig. 10. The solid curves denote differences based upon comparisons with the modified Keller box method applied for η_{max} of 8 for $\beta = 0.5$ and of 10 for $\beta = -0.1$. The dotted curves denote differences based upon comparisons with the basic Keller box method applied at corresponding η_{max}. For solutions obtained with η_{max} less than 8 for $\beta = 0.5$ and η_{max} less than 10 for $\beta = 0.1$, the differences were obtained on the range of the basic comparison solutions by extending the solutions using the asymptotic solution for the modified Keller box method and using (53) for the basic Keller box method. These solutions exhibit the same features as the flat plate solutions.

In the process of obtaining the solutions with pressure gradient, it was apparent that the coefficients in (32), (33), (39) and (40) diverge and that the series will diverge for finite ξ and infinite series. Therefore, it was necessary to truncate the series at the point (i value) where the series starts to diverge with given ξ. Then, as ξ becomes smaller, the number of terms in the truncated series decreases and the error increases. The magnitude of this error was monitored and the ξ corresponding to η_{max} is in the range of 1 to 2.5 when the errors become larger than 10^{-2}. For such small ξ, the series was truncated after a few terms (actually with only 1 term for the largest errors) to prevent divergence and greater errors should be expected. It is interesting to note that the RMS error of Fig. 9 and the RMS difference of Fig. 10 can be reasonably small even when the errors in $F_p(\xi)$ and $G_c(\xi)$ become relatively large.

A more detailed derivation of the asymptotic solution and the box method is presented in Ref. [8]. The complete computational results are also reported.

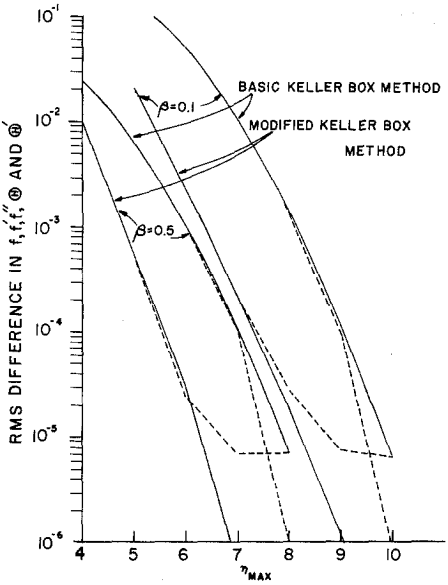

FIG. 10. The RMS difference in the converged solutions for the velocity and temperature profiles with $\gamma = 1.4$, $M = 4$, $C_n = \frac{1}{2}$, $F_\infty = 1 = f'_\infty$, $P_R = 0.75$, $\Theta_\infty = \Theta_w = l = 1$, and $\beta = 0.5$ and -0.1 on the interval 0 to 8 for $\beta = 0.5$ and 0 to 10 for $\beta = -0.1$.

CONCLUSIONS

The author is grateful to the reviewers for pointing out that Sills [9, 10] has applied several transformations to transform the semi-infinite and infinite flow regions of several boundary flows into finite regions such that "outer" boundary conditions could be imposed properly. This technique has not been applied or evaluated in this investigation. One reviewer points out that "transformation of a semi-infinite interval to [0, 1] introduces a singularity at $x = 1$, and this is not always a bargain. In many cases in which such transformations are used, an asymptotic expansion must be used near $x = 1$ in order to get the solution away from the singular pont." The most important observation in considering application of Sill's method or the present method is that the present method results in a reduction instead of an addition in the number of computation points.

It is apparent from the present investigation that use of the asymptotic solution has at least three significant advantages:

1. The required range of η for calculation can be reduced for many problems with significant saving in computer time.

2. The accuracy of the solution may be improved significantly.

3. The estimate of η_{max} for calculations becomes less critical for cases where guidelines may not be known. As a result it is possible to err on the low side for this estimate.

As a final observation it should be noted that the technique presented here does not have unique application to the Keller box method. It should be applicable to any of the iterative techniques discussed by Blottner [3, 4] and may have even wider application.

The minor increase in computer time (6.7% for the same η_{max} in both algorithms) is apparently just the time required to compute the constants for the asymptotic solution from the new iterates after each iteration and to compute the special functions in the asymptotic solution. However, the major advantage of including the asymptotic solution is that computer time can be reduced (25%) by reducing the computation range (i.e., smaller η_{max}) without sacrifice in accuracy of the solution. Furthermore, the resulting solution can be extended accurately far beyond the basic computation region.

ACKNOWLEDGMENTS

This research was supported by ONR Contract N00014-77-C-0257 (monitored by Mr. Morton Cooper) and by the Computer Science Center at the University of Maryland. The comments and suggestions of the reviewers of this paper have also been very helpful.

REFERENCES

1. H. B. KELLER, *in* "Numerical Solutions of Partial Differential Equations" (B. Hubbard, Ed.), Vol. 2, pp. 327–350, Academic Press, New York, 1970.
2. H. B. KELLER, *in* "Annual Reveiw of Fluid Mechanics" (M. VanDyke, J. V. Wehausen, and J. L. Lumley, Eds.), Vol. 10, pp. 417–433, 1978.
3. F. G. Blottner, *in* Short Course "Computational Methods for Inviscid and Viscous Two and Three Dimensional Flow Fields," sponsored by AGARD at the von Karman Institute for Fluid Dynamics and the Fluid Dynamics Institute, Hanover, New Hampshire, 1975.
4. F. G. BLOTTNER, *in* "Computer Methods in Applied Mechanics and Engineering," Vol. 6, pp. 1–30, North-Holland, Amsterdam, 1975.
5. M. VANDYKE, "Perturbation Methods in Fluid Mechanics," Academic Press, New York/London, 1964.
6. L. PRANDT, *in* "Aerodynamic Theory" (W. F. Durand, Ed.), pp. 84–87, 1943.
7. H. SCHLICHTING, "Boundary-Layer Theory," McGraw–Hill, New York, 1968.
8. [illegible] No. AE 80-1, Dept. of Aerospace Eng., University of Maryland, 1980.
9. J. A. SILLS, "The Effect of Boundary-Layer Separation on Laminar Heat Transfer," M.S. thesis, Georgia Institute of Technology, February 1967.
10. J. A. SILLS, *AIAA J.* **7**, No. 1 (January 1969), 117–123.